RESEARCH ARTICLE OPEN ACCESS

Polypyrrole/PZT Thermistor: An Effective pre-cursor towards sensor design

S.N. Paul[1], Vineet V. Karambelkar[2*], J.D. Ekhe[3]
[1](Department of Metallurgical and Materials Engineering, Visvesvaraya National Institute of Technology, Nagpur-10, India)
[2*](Department of Metallurgical and Materials Engineering, Visvesvaraya National Institute of Technology, Nagpur-10, India.)
[3](Department of Chemistry, Visvesvaraya National Institute of Technology, Nagpur-10, India.)

Abstract
Pristine Polypyrrole was prepared by employing inverse emulsion polymerization technique using Methanesulfonic acid as a dopant and sodium lauryl sulfate (SLS) as a surfactant. Oxidizing agent used was Potassium Persulfate. An attempt was made to formulate a Polypyrrole device by blending Polypyrrole with Lead Zirconate Titanate (PZT) piezoceramic powder which showed characteristics akin to a Thermistor thereby formulating its use as a pre-cursor to a temperature sensor upon Current vs. Voltage as well as Temperature vs. Conductivity studies. Characterization studies of Polypyrrole/PZT blends using Fourier Transform Infrared Spectra, Scanning Electron Microscopy and X-ray diffraction studies yielded satisfactory and confirmatory results. Extensive conductivity studies were carried out from 298 K - 383 K and Conductivity as high as 3.97 $S \bullet cm^{-1}$ was obtained at a surfactant and dopant concentration of 9.0 g and 11.0 g respectively. Liquid Phase Sintering of Ppy/PZT blends with Tin (Sn) metal powder offers exciting opportunity towards formulation of a temperature sensor, the diffusivity studies of which are still underway.

Keywords: Polypyrrole; PZT; Inverse Emulsion Polymerization; Thermistor; Sensor; Liquid Phase Sintering.

I. Introduction

Several electrically conducting polymers have been studied due to their exclusive physical properties and interesting applications. Of all these polymers, polypyrrole (PPy) is one of the most extensively studied conducting polymer. Polypyrrole is a fused five membered heterocyclic ring compound which has an excellent potential as organic semiconductor and a potential anti-tumor agent [1]. Polypyrrole is the most thoroughly investigated conductive polymer due to its unique blend of properties (air stability and electrochemical stability, and having a low band gap [2]. Polypyrrole finds applications such as electrical conductors, nonlinear optical devices, photoresists, solar cells and transistors [3].

Unlike traditional organic synthesis routes of substituted fused five membered heterocyclic rings which often result in a low yielding product due to ring strain of the fused five rings [4], the chemical oxidative (emulsion) polymerization of pyrrole is a facile synthesis route for producing polypyrrole on a large scale. The emulsion polymerization process has many unique advantages. The physical state of the emulsion system makes the reaction process control very easy. Thermal and viscosity stability is attained quite effortlessly and the product obtained is mostly pure and can be used even without refining. Very high reaction rates can be attained by this technique. Emulsion polymerization is an exclusive process in that the polymer molecular weight is increased without affecting the reaction rate (kinetics). Nowadays, micro-emulsion polymerization and inverse emulsion polymerization techniques have gained significant attention with respect to the preparation of polyaniline and polypyrrole [5]. In this, solution of a hydrophilic monomer is emulsified in a non-polar organic solvent such as chloroform and polymerization is initiated with an oil-soluble initiator.

Inverse emulsion polymerization has been traditionally applied in various commercial polymerizations and co polymerizations of acryl amide as well as other water soluble monomers.

Traditional organic synthesis routes for synthesizing fused thiapentalenes like the Dieckmann Condensation [6], Selegue's route [7] or Snyder's route [8] suffer from a few drawbacks like inordinately low yields, difficult to remove impurities and use of toxic and regulated reagents.

In contrast, polymerization process, particularly chemical oxidative polymerization is a convenient and facile method to synthesize these fused ring compounds. The main advantage of chemical method is large scale production of the polymer at an affordable cost along with enhanced conductivity.

In this paper an attempt was made to synthesize Polypyrrole, an intrinsically conducting polymer

(ICP) via chemical oxidative polymerization method or inverse emulsion polymerization method. One of the main advantages of using pyrrole as the monomer is its low oxidation potential thus facilitating the trial and use of a variety of oxidizing agents and solvents for polypyrrole synthesis. Synthesis of Polypyrrole was facilitated using Methanesulfonic acid as a dopant along with Potassium persulfate as an oxidant in addition to Sodium Lauryl Sulfate as a surfactant. High conductivity of up to 3.97 $S \bullet cm^{-1}$ was obtained at 298 K at 9.0 g and 11.0 g concentration of surfactant and dopant respectively. The pristine polymer was blended with Lead Zirconate Titanate (PZT) a piezoceramic powder and a Thermistor like device was fabricated which was found to behave like a pre-cursor to a temperature sensor.

II. Experimental Part

All the reactions were carried out using standard laboratory apparatus unless otherwise noted. Pyrrole monomer (Acros) 99.9% extra pure, organic reagents like chloroform (Fischer Scientific) (99.9% extra pure), Acetone (Fischer Scientific) (Analar grade, 99% pure), dopant Methanesulfonic acid, and surfactant Sodium Lauryl Sulfate (National Chemicals, India) along with oxidant Potassium persulfate (Qualigens Fine Chemicals, India) were used as received. Lead Zirconate Titanate (PZT) piezoceramic powder (M/s. Sparkler Piezoceramics Pvt. Ltd., Pune, India) having a particle size of 950 nm measured on a Fischer Sub-sieve Sizer, Fsss) was used as received. Fourier transform infra red (FTIR) spectra were recorded using a Perkin-Elmer SPECTRUM ONE system, X-ray diffraction studies were carried out using a PANalytical XPERT-PRO X-ray diffractometer with CuK_{α} radiation of wavelength 1.5406 Å with a continuous scan speed of 0.045^{0} per minute. Scanning Electron Microscope (SEM) JEOL 6380 A was used to take the micrographs of pristine Polypyrrole and PPy/PZT blends. Resistance measurement of polypyrrole was carried out on a two probe connected to a Mastech digital multimeter (Model MAS 830L). Hydraulic KBr pellet press was used to prepare Ppy/PZT/Sn "green" powder compacts. Therelek furnace with a maximum temperature range of 1000^{0}C was used to sinter the "green" pellets.

2.1 Polymerization Procedure

2.1.1 Synthesis of polypyrrole by inverse emulsion polymerization

In a 250 ml conical flask was taken a mixture of methanesulfonic acid dopant (4 ml, 5.92 g) and water (20 ml). Pyrrole monomer (1.2 ml, 1.16 g) dispersed in water (30 ml) was added to the above mixture and constantly stirred at 293 K. Sodium lauryl sulfate surfactant (1.0 g) dispersed in water (20 ml) and Potassium persulfate initiator (3.0 g) dispersed in Chloroform (30 ml) were added drop wise to the stirring reaction mixture. The reaction mixture was allowed to stir constantly for one hour duration, after which it was poured in acetone to precipitate the black colored polymer. The polymer was washed with water, dried in an oven at 373 K, and weighed until a constant weight was maintained.

2.2 Formulation of a Polypyrrole/PZT device

A simple glass tube was cut into a piece of approximately 4 inches in length. Polypyrrole powder along with PZT powder in the molar ratio of 60:40 was filled into it, and a copper wire was inserted into the bore of the cut glass piece at both the ends such that the two ends of the wire just touch each other. Small pieces of silver wire were placed at both the ends such that a sort of a non-rectifying metal-semiconductor ohmic contact was formed wherein silver wire acted as cathode and copper wire acted as anode. The two ends of the tube were then sealed using a quick fix adhesive having a relatively high melting point (> 623 K).

Resistance measurements were then taken on a two point probe Keithley digital multimeter and conductivity was determined using the mathematical relation: C = 1/R.

III. Results and Discussion

Polymerization was carried out for different variations such as surfactant strength, acid strength, oxidizing agent, reaction temperature and time. Reaction parameters were evaluated individually, to study optimum conductivity obtainable for Polypyrrole. It was found that Polypyrrole being insoluble in most of the organic solvents was infusible which restricted its processing and applications in commercial fields [9-10]. To overcome this hitch, a novel method was devised to measure the conductivity of polypyrrole by blending the pristine polymer with Lead Zirconate Titanate (PZT) piezoceramic powder. Scheme 1 depicts the method whereby a Polypyrrole device was formulated.

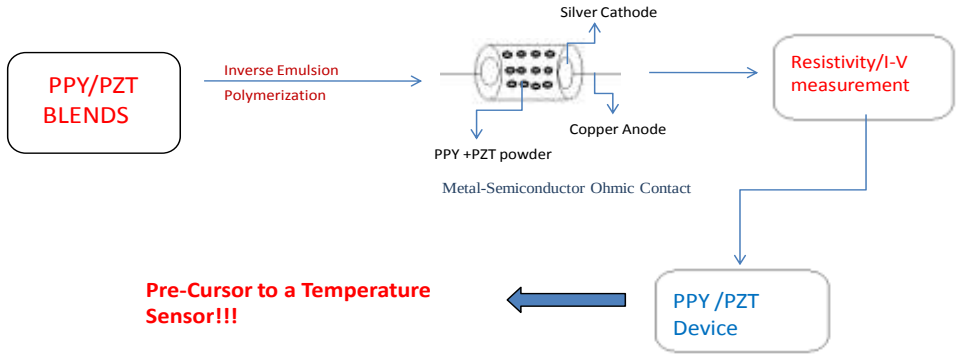

Scheme 1: Formulation of a PPy/PZT Device

Resistance studies of this Polypyrrole device at room temperatures (23^0C-26^0C) and at elevated temperatures up to 110^0C revealed some interesting trends regarding the conductivity point of view. Conductivity as high as 3.97 S•cm^{-1} was obtained at surfactant and dopant concentration of 9.0 g and 11.0 g respectively. Likewise, every reaction process parameter was varied to study variations in conductivity values between 298 K and 383 K. The effects of concentrations of various process parameters with respect to the conductivity obtained are summarized in Fig's. 1-6. Conductivity steadily decreased below 298 K as well as above 383 K.

(i) **Effect of varying monomer concentrations on conductivity:**

Maximum conductivity (σ) obtained at 298 K was 3.80 S/cm, reached a maximum, and then decreased. At 383 K conductivity was 1.40 S/cm, even at high monomer concentrations. Conductivity consistently decreased with increasing temperatures. Table 1 summarizes conductivities obtained at 298 K and 383 K.

Table 1: Conductivities for various Monomer concentrations at 298 K and 383 K

Monomer Concentration (ml)	Conductivity (σ) at 298 K	Conductivity (σ) at 383 K
1	0.90	0.70
2	0.95	0.88
3	1.90	1.40
4	0.32	0.21
5	1.10	0.72
6	3.80	0.95

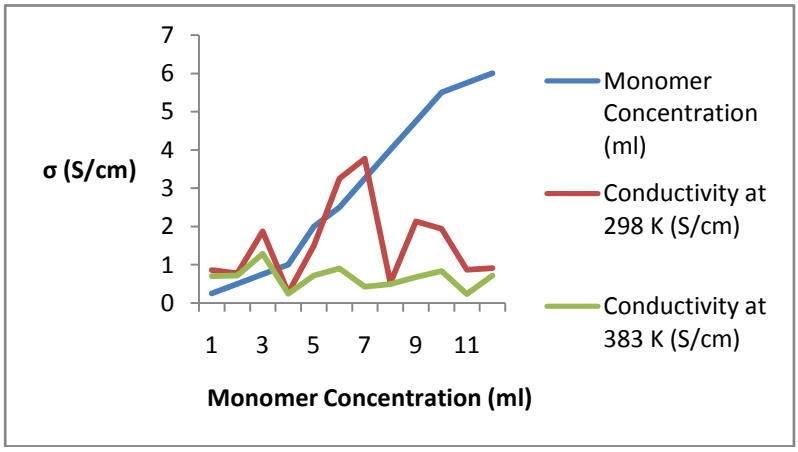

Figure 1: Conductivities of Polypyrrole blends for variable Monomer concentrations

(ii) **Effect of varying surfactant concentrations on conductivity:**

Maximum conductivity (σ) obtained at 298 K was 3.97 S/cm, reached a maximum, and then decreased. Sudden sharp increase in conductivity can be attributed to the formation of a conducting path which could have been formed, thus facilitating the flow of current. At 383 K conductivity was 1.30 S/cm. In case of increasing surfactant concentrations, too, conductivity decreased with increasing temperatures. Table 2 lists the conductivities at 298 K and 383 K for variable surfactant concentrations.

Table 2: Conductivities for various Surfactant concentrations at 298 K and 383 K

Surfactant Concentration (ml)	Conductivity (σ) at 298 K	Conductivity (σ) at 383 K
1	0.81	0.62
2	0.73	0.58
3	1.90	1.30
4	0.45	0.12
5	0.97	0.82
6	0.48	0.45
7	0.51	0.47
8	0.83	0.46
9	3.97	0.75

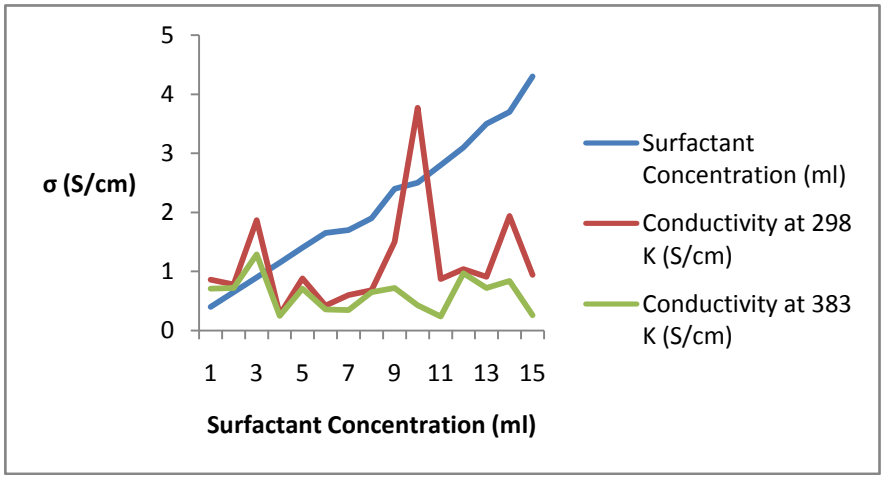

Figure 2: Conductivities of Polypyrrole blends for variable Surfactant concentrations

(iii) **Effect of varying oxidant concentrations on conductivity:**
Maximum conductivity (σ) obtained at 298 K was 3.77 S/cm, reached a maximum, and then drastically decreased to 0.95 S/cm as seen from the graph. At 383 K, maximum conductivity obtained was 1.32 S/cm. As in the case of monomer and surfactant, conductivity decreased with increasing temperatures. Table 3 outlines conductivities obtained at 298 K and 383 K for varying oxidant concentrations.

Table 3: Conductivities for various Oxidant concentrations at 298 K and 383 K

Oxidant Concentration (g)	Conductivity (σ) at 298 K	Conductivity (σ) at 383 K
1	0.97	0.82
2	0.87	0.83
3	1.97	1.32
4	0.71	0.23
5	0.82	0.78
6	0.55	0.48
7	0.85	0.84
8	0.92	0.49
9	0.93	0.22
10	1.82	0.91
11	0.96	0.98
12	1.30	0.99
13	3.77	0.97

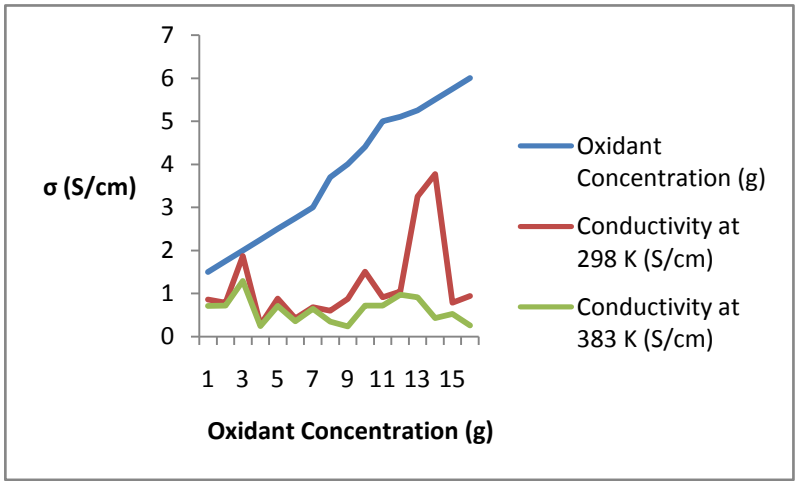

Figure 3: Conductivities of Polypyrrole blends for variable Oxidant concentrations

(iv) **Effect of varying dopant concentrations on conductivity:**

Maximum conductivity obtained at 298 K was 3.97 S/cm, reached a maximum, and then decreased steeply to 0.34 S/cm as seen from the graph. This steep decrease in conductivity value can be attributed to increased amount of dopant on the polymer backbone chain. Table 4 gives the conductivities obtained for varying dopant concentrations at 298 K and 383 K.

Table 4: Conductivities for various Dopant concentrations at 298 K and 383 K

Dopant Concentration (ml)	Conductivity (σ) at 298 K	Conductivity (σ) at 383 K
1	1.21	0.93
2	1.00	0.76
3	1.98	1.47
4	0.33	0.12
5	1.10	0.80
6	1.76	0.32
7	1.99	1.32
8	1.25	0.36
9	0.36	0.24
10	3.22	0.97
11	3.97	0.32

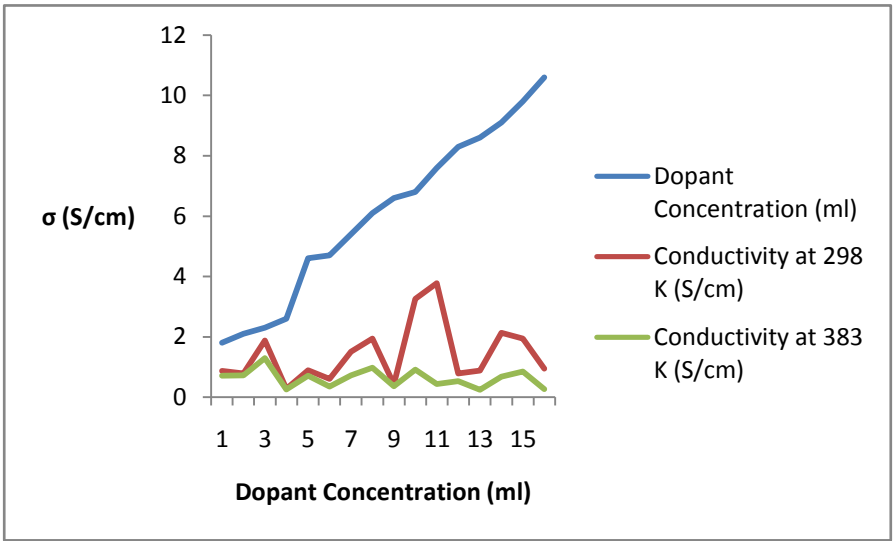

Figure 4: Conductivities of Polypyrrole blends for variable Dopant concentrations

(v) **Effect of varying temperatures on conductivity:**

At 298 K conductivity as high as 3.80 S/cm was observed, and at 383 K conductivity obtained was drastically low at 0.70 S/cm as seen from the graph. Fig. 5 summarizes conductivity of polypyrrole blends for variable temperature ranges.

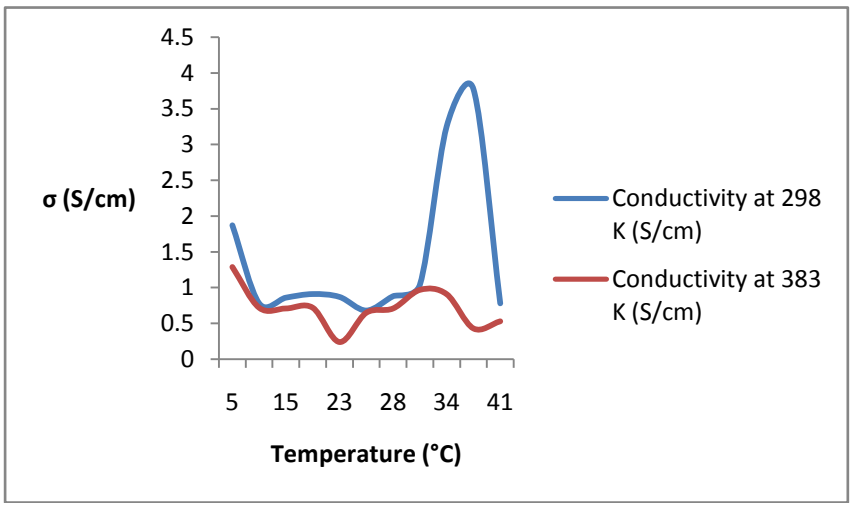

Figure 5: Conductivities of Polypyrrole blends for variable Temperature Ranges

(vi) **Effect of varying stirring times on conductivity:**

Varying stirring times yielded conductivity as high as 1.87 S/cm at 1.0 hour of stirring time at 298 K and dropped to 1.29 S/cm as observed from the graph. At 383 K, lowest conductivity obtained was 0.25 S/cm at 3.5 hours of stirring. Higher stirring times, however, yielded negligible conductivity values. Fig. 6 illustrates the graph of conductivities obtained against variable stirring times at 298 K and 383 K.

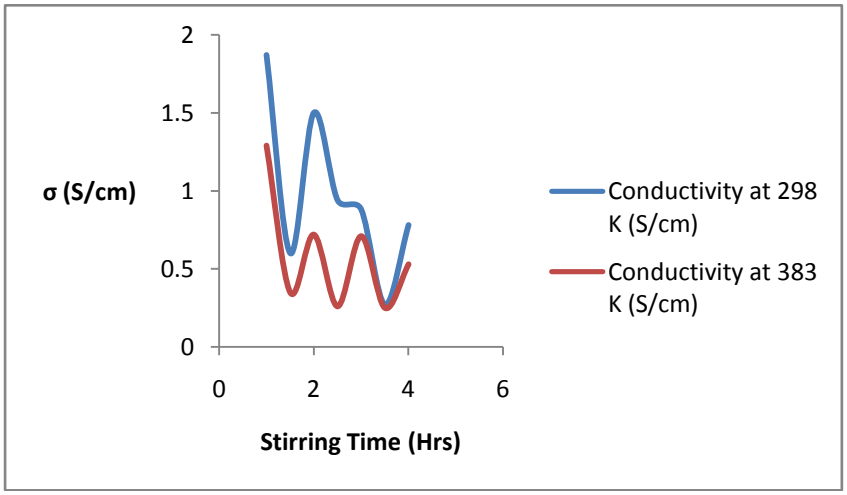

Figure 6: Conductivities of Polypyrrole blends for variable Stirring Times

3.1 Temperature vs. Conductivity Curves of PPy/PZT blends – Arrhenius Plots

Arrhenius plots of PPy/PZT blends are summarized in Fig. 7. A study of the graphs at room temperatures (23^0C-26^0C) and at elevated temperatures showed a **linear** relationship between temperature and resistance indicative of the relation,

$\Delta R = k\Delta T$

Where, ΔR = change in resistance

ΔT = change in temperature

k = first-order temperature coefficient of resistance

Curves indicated that the device seemed to behave similar to a **Thermistor** which is a type of resistor whose resistance varies with different temperatures and is widely used in temperature sensors. When the PPy/PZT device was in the cold condition (i.e. at room temperature) resistance was found to be high, on the contrary when the device was heated, resistance drastically dropped with rising conductivity.

Since the measured temperature range is small (273 K – 373 K), i.e. from 0^0C to 100^0C, first order linear approximation seems to have worked best.

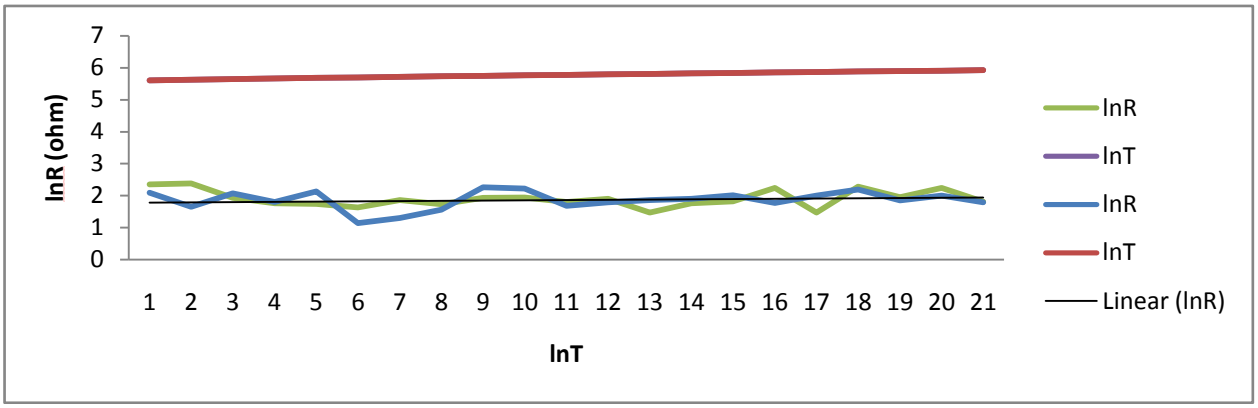

Figure 7: Arrhenius Plots of PPy/PZT blends Device at Room Temperatures (23^0C-26^0C) and at Elevated Temperatures

3.2 Temperature vs. Conductivity Curves of PPy/PZT blends

Temperature vs. Conductivity curves were studied at three different stages of temperatures; i.e. at low temperatures (0^0C-15^0C), moderate temperatures (20^0C-25^0C), high temperatures (30^0C-35^0C) and very high temperatures (40^0C-45^0C). The curves are summarized in Fig. 8 and Fig. 9

Solid line in the graphs indicated linear regression analysis of the experimental data. Graphs indicated increase in conductivity as temperature increased. However, at higher temperatures conductivity decreased. Decrease in conductivity indicated resistance which was an **ideal requirement** for a temperature sensor. It can be assumed that the "Thermistor" sort of device which was construed could be effectively used as a **precursor to a temperature sensor**.

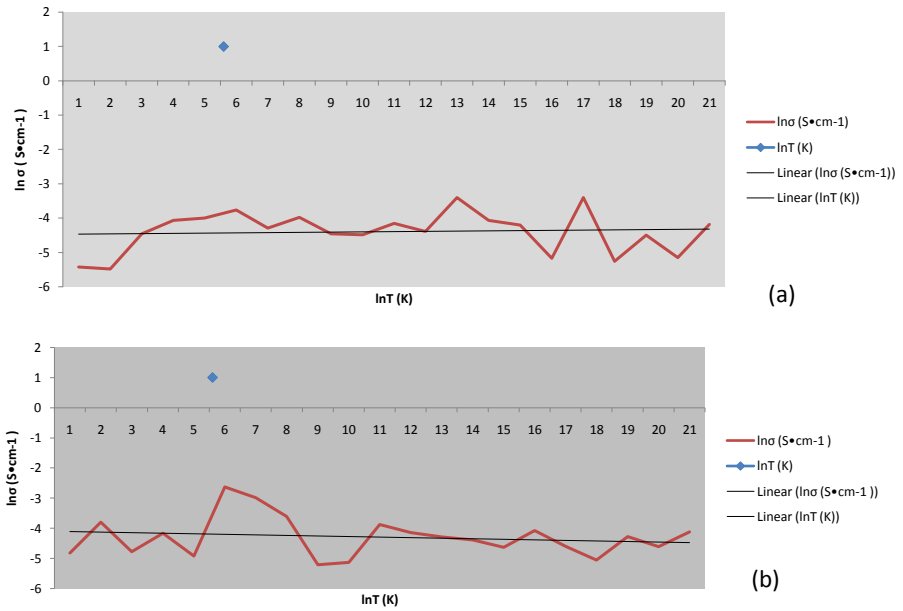

Figure 8: Temperature vs. Conductivity Curves of PPy/PZT blends- (a) Low Temperatures, 0^0C-15^0C and (b) Moderate Temperatures, 20^0C-25^0C

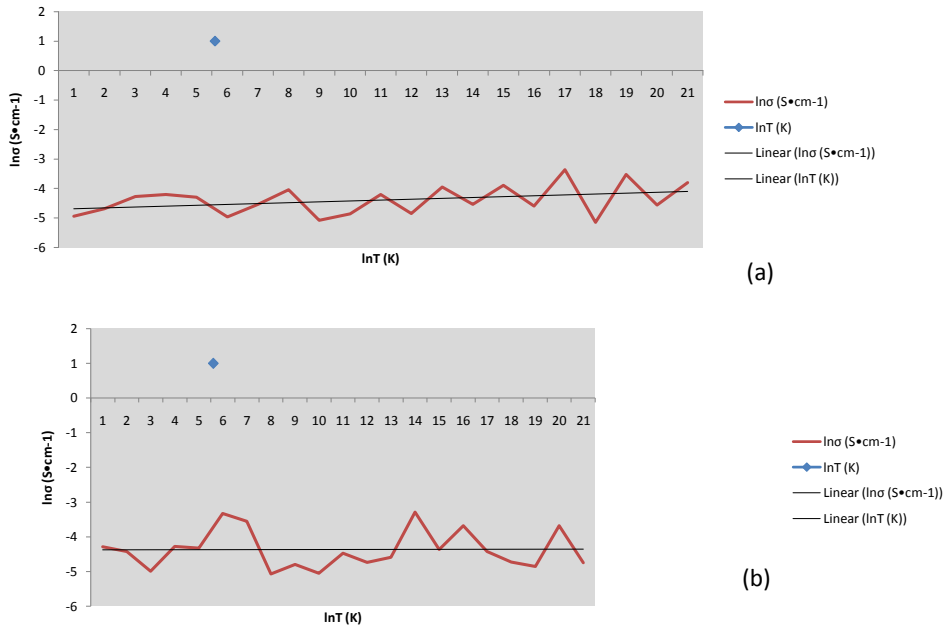

Figure 9: Temperature vs. Conductivity Curves of PPy/PZT blends- (a) High Temperatures, 30^0C-35^0C and (b) Very High Temperatures, 40^0C-45^0C

3.3 Current-Voltage (I-V) Curves of PPy/PZT blends

I-V curves of the PPy/PZT device are depicted in Fig's.10 and 11. Analysis of the graphs further confirmed the effectiveness of this polymer device as a **temperature sensor.** When the device was in cold condition (room temperature), voltage signal increased and resistance rised. As the temperature increased, voltage signal decreased and the resistance dropped. From the graphs it was evident that when a large current set in, non linearity increased, leading to joule heating.

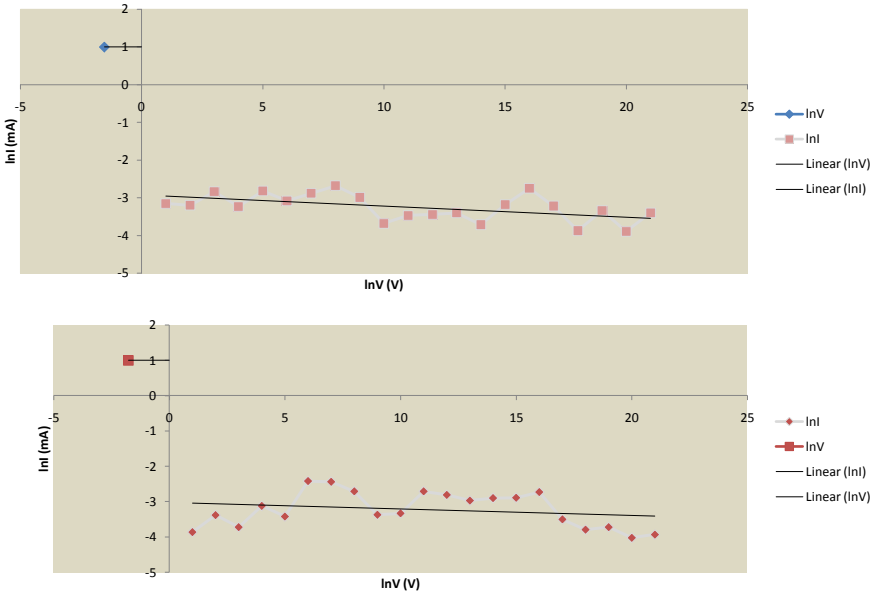

Figure 10: Current-Voltage (I-V) Curves of PPy/PZT blends (When device is in cold condition,i.e. at room temperature, without heating)

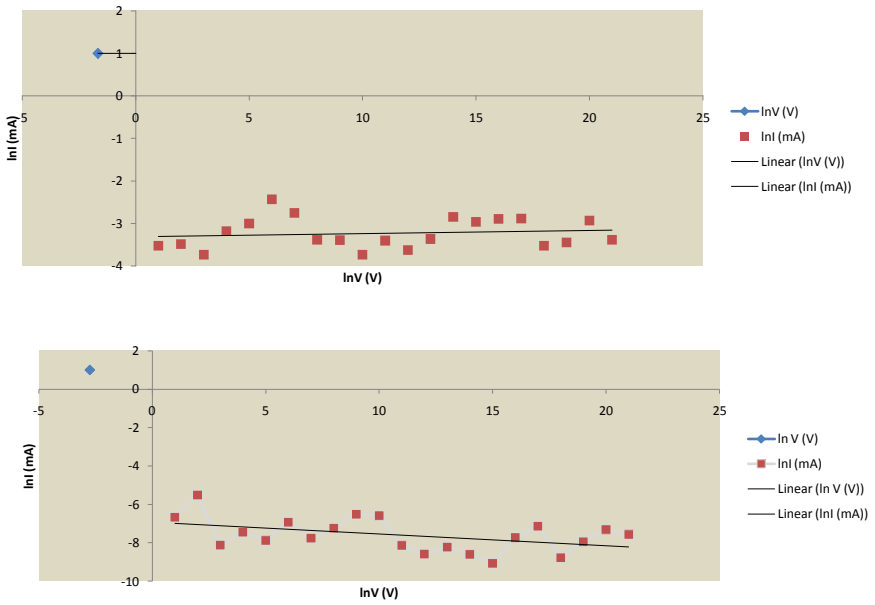

Figure 11: Current-Voltage (I-V) Curves of PPy/PZT blends (When device is in hot condition)

3.4 Powder Compaction and Liquid Phase Sintering of the "Green" Compacts

Liquid Phase Sintering is a consolidation technique of powder compacts containing more than one component at a temperature above the solidus of the components and hence in the presence of a liquid. Unlike solid state sintering, the microstructure change during liquid phase sintering is fast because of fast material transport through the liquid. As a liquid phase forms during heating of powder mixture compact, liquid flows into fine capillaries due to the capillary pressure difference between the fine and coarse channels between solid particles and these solid particles can be redistributed by this liquid flow. A few advantages of liquid phase sintering include, a lack of backstress problem, unlike in solid state sintering, since liquid phase is present between the solid grains. Since the pore filling occurs as a result

of grain growth, the sintering time for densification is governed by grain growth kinetics and hence fast densification is ensured due to formation of intrinsic pores at the sites of liquid forming particles when they melt, since the melt is sucked out between the solid particles by capillary action and a high final density is ensured and resulting microstructures often provide mechanical and physical material properties superior to solid state sintered materials.

Keeping these advantages in mind, PPy/PZT blends were further blended with Tin (Sn) metal powder which was supposed to act like a liquid phase between PPy and PZT solids, and the resulting PPy/PZT/Sn blends were powder compacted in a hydraulic KBr pellet press, employing the traditional Powder Metallurgy route to yield the actual sensor. Scheme 2 illustrates the process flow chart for the actual PPy/PZT sensor formulation. Figure 12 summarizes the actual powder compaction technique and Figure 13 depicts the actual PPy/PZT sensor, diffusivity studies of which are still underway. Figure 14 (a) shows the SEM micrograph of pre-sintered PPy//PZT/Sn pressed powder compact whereas (b) shows the SEM micrograph depicting the distribution of Liquid Sn between spherical particles of PPY/PZT with an intermediate liquid film (post-sintered). Further detailed diffusivity studies of this sensor are still en route. However, characterization of the sensor is reported herein.

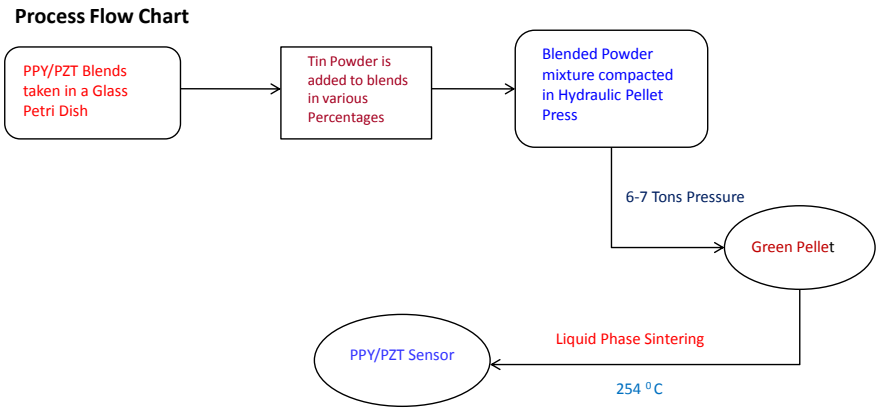

Scheme 2: Formulation of a PPy/PZT Sensor

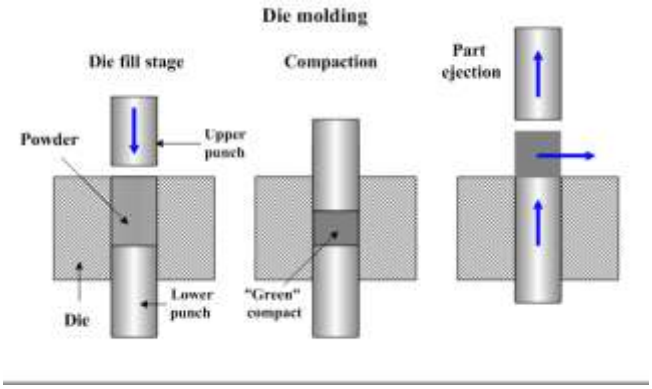

Figure 12: Actual Powder Compaction Process

Figure 13: The actual PPy/PZT Sensor

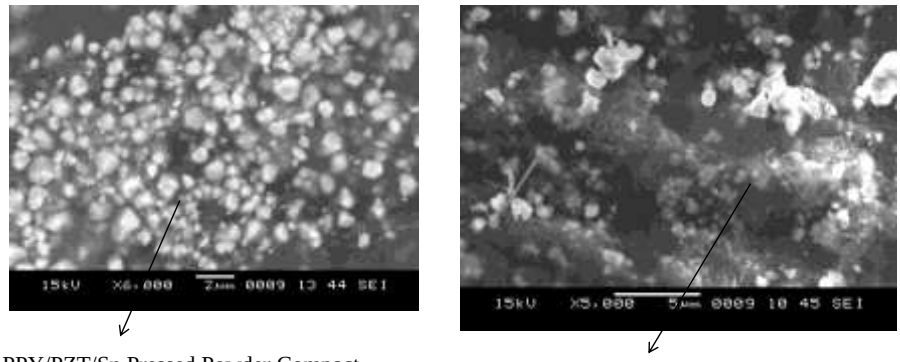

Figure 14: (a) SEM micrograph of pre-sintered PPy//PZT/Sn pressed powder compact. (b) SEM micrograph depicting the distribution of Liquid Sn between spherical particles of PPY/PZT with an intermediate liquid film (post-sintered)

3.5 Characterization of the PPy/PZT Sensor

3.5.1 Fourier Transform Infrared (FT-IR) spectra: FT-IR spectra of a few PPy/PZT blends showed the following trends:

FTIR spectra of a PPy/PZT blend showed characteristic peaks at:

3710,3699,3696 and 3698 cm^{-1} (N-H str) ; 2924,2854,2921 cm^{-1} (C_{sp2} – H str) ; 1539 and 1538 cm^{-1} (C=C); 1205, 1216 and 1219 cm^{-1} (C-N); 1047 and 1051cm^{-1} (=C-H in plane vibration); 636,629,626 and 652 cm^{-1}(C-Br).

FTIR spectra of another PPy/PZT blend showed characteristic peaks at:

1715 cm^{-1} corresponding to zirconium oxide, 3440 cm-1 corresponding to titanium oxide and 3699 cm^{-1} corresponding to lead oxide which was also similar to N-H stretch indicating adsorption of PZT on Polypyrrole when concentration of PZT was more as compared to other blends .

As the concentration of PZT powder decreased, peaks of Ppy and PZT didn't coincide. Figure 15 depicts the FT-IR graphs of PPy/PZT blends.

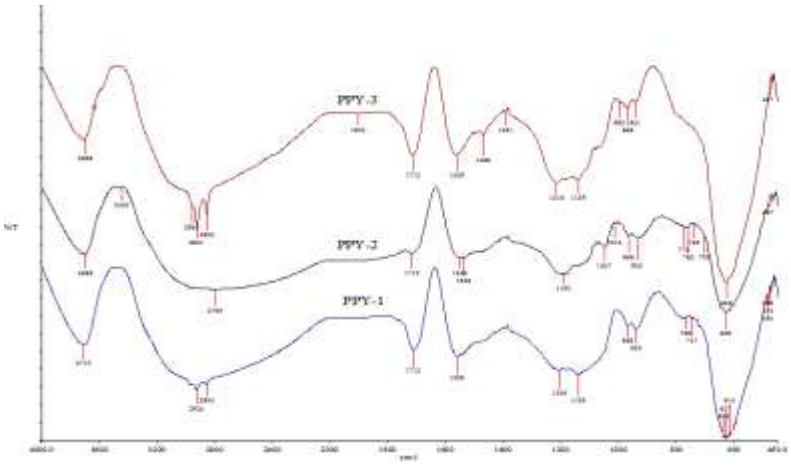

Figure 15: FT-IR Spectra of PPy/PZT blends

3.5.2 X-Ray diffraction (XRD) Studies:

Ideal 2θ peak values for pure Ppy as well as PZT range between 10^0 to 30^0. Relative peak intensity of 100% was found at $2\theta = 31^0$ in PPy doped with PZT which clearly indicated that PPy was *in situ* polymerized with PZT. Figure 16 depicts the XRD graphs of PPy/PZT blends.

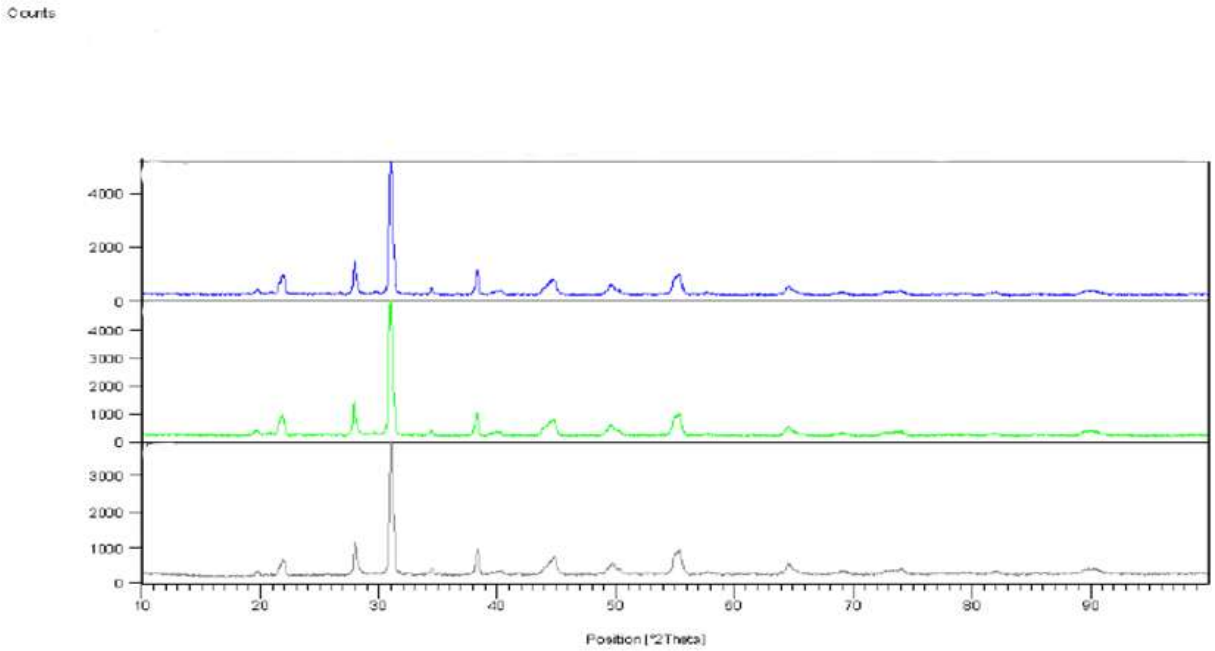

Figure 16: XRD spectrum of PPY/PZT blends

3.5.3 Scanning Electron Microscopy/Energy Dispersive X-Ray Spectroscopy (SEM/EDX) Studies:

Fig.'s 17-19 illustrates a few SEM micrographs of PPy/PZT blends. Analysis of SEM/EDX data suggested that the refinement of PPy chains was specifically related to the Pb (lead) content of the PZT powder. The lesser the PZT powder, the lesser refinement of the PPy chains was found.

In the **blend I**, C and N in K-shell was 1.61 and 0.00 wt % respectively. In the L-shell, Zr and Ti were 7.37 and 2.34 wt % respectively. In the M-shell, Pb was 39.25 wt % which indicated that as the pyrrole monomer concentration was relatively much lesser than that of PZT, there was more refinement in the polypyrrole chain and molecules. In the **blend II**, similarly, C and N in the K shell was 5.48 and 0.00 wt% respecrively. In the L-shell, Zr and Ti were 18.29 and 16.27 wt% respectively. In the M-shell, Pb was 34.26 wt % . Concentration of Pyrrole monomer was even lesser but concentration of PZT was lesser than in blend I. However, as the concentration of PZT powder was decreased, in **blend III**, Pb content in M-shell was 0.00 wt % and C wt % in K-shell shot up to 86.14 wt %, indicating less adsorption on PPy chains, hence conductivity decreased.

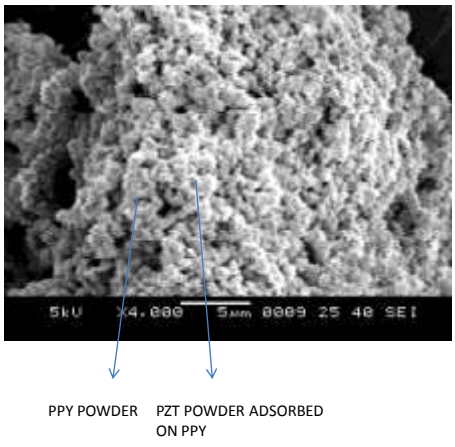

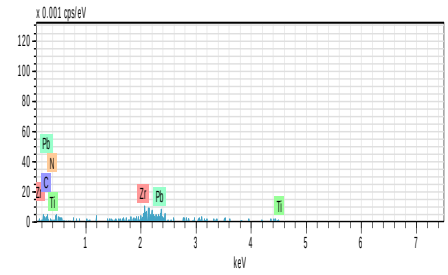

El	AN	Series	unn. C [wt.%]	norm. C [wt.%]	Atom. C [at.%]	Error (1 Sigma) [wt.%]
Pb	82	M-series	39.25	77.61	41.78	11.89
Zr	40	L-series	7.37	14.57	17.82	3.96
Ti	22	L-series	2.34	4.63	10.79	12.57
C	6	K-series	1.61	3.19	29.62	4.56
N	7	K-series	0.00	0.00	0.00	0.00
		Total:	50.57	100.00	100.00	

Figure 17: SEM Micrographs of PPy/PZT blends with EDX Data

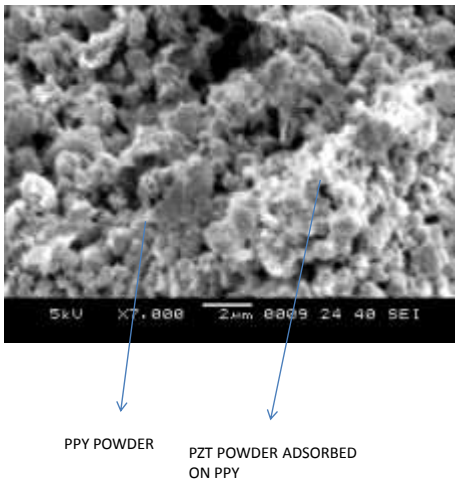

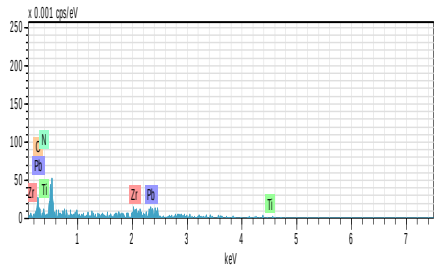

El	AN	Series	unn. C [wt.%]	norm. C [wt.%]	Atom. C [at.%]	Error (1 Sigma) [wt.%]
Pb	82	M-series	34.26	46.11	14.23	4.90
Zr	40	L-series	18.29	24.62	17.26	2.79
Ti	22	L-series	16.27	21.89	29.24	13.61
C	6	K-series	5.48	7.38	39.27	3.62
N	7	K-series	0.00	0.00	0.00	0.00
		Total:	74.30	100.00	100.00	

Figure 18: SEM Micrographs of PPy/PZT blends with EDX Data

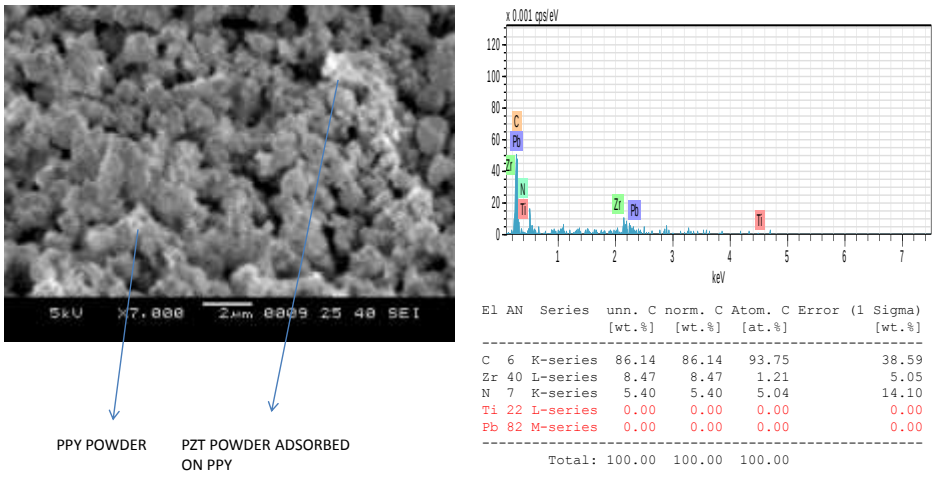

Figure 19: SEM Micrographs of PPy/PZT blends with EDX Data

IV. Conclusions

Polypyrrole, an intrinsically conducting polymer was prepared via inverse emulsion polymerization method and electrical conductivity as high as 3.97 S•cm^{-1} was obtained by blending with Lead Zirconate Titanate (PZT) piezoceramic powder. A Thermistor-like device was formulated with these PPY/PZT blends and it was confirmed by I-V studies and Temperature/Voltage studies. Liquid phase sintering was successfully employed to form Polypyrrole/PZT pellets with Tin metal powder as an intermediate liquid phase to yield the final temperature sensor, diffusivity studies of which are still on.

References

[1] S. Kwon, T. Hong, S. Kim, J. Jeong, J. Hahn, J. Jang, Biosens. Bioelectron. 25, (2010) 1307-1312.
[2] T. Fransto, A. Garcia, Superficieś y vacio. 22 (2009) 15-19.
[3] U. Abaci, Y. Guney, U. Kadiroglu, Electrochim. Acta. 96 (2013) 214-224 .
[4] Y. Hong, B. Feng, G. Liu, S. Wang, H. Li, J. Ding, Y. Zeng, D. Wei, J. Alloy Comp. 476 (2009) 612-618.
[5] L. Yang, B. Weng, Synth. Met. 159 (2009) 2249-2252.
[6] W. Dieckmann**,** Ber. Dtsch. Chem. Ges., 27 (1894) 2475–2477.
[7] C. A. Snyder, J. P. Selegue, E. Dosunmu, N. C. Tice, S. Parkin, J. Org. Chem. 68 (2003) 7455-7459.
[8] C. A. Snyder, J. P. Selegue, N.C. Tice, C. E. Wallace, M.T. Blankenbuehler, S. Parkin, K.D.E. Allen, J.Am.Chem.Soc. 127 (2005) 15010-15011.
[9] A.T. Lawal, G.G. Wallace, J. Appl.Sci. 8 (2008) 2967-2974.
[10] D.V. Brezoi, J.Sci.Arts. 12 (2010) 53-58.